A Simulation Study of Flow and Pressure Distribution Patterns in and around of Tandem Blade Rotor of Savonius (TBS) Hydrokinetic Turbine Model

B. Wahyudi, S. Soeparman, S. Wahyudi, and W. Denny.

***Abstract*—The performance of hydrokinetic turbines of Savonius using a Tandem Blade Savonius (TBS) rotor was studied. These were three types of TBS: Overlap (Type I), Symmetrically (Type II) and Convergence (Type III). Through a comprehensive bibliographical research, it is possible to identify the influenced parameters, and to show that the optimum efficiency of the Savonius rotor can be particularly improved their partition space between blade and tandem. This simulation shows the way of the flow characteristic and pressure distribution pattern in and around of the blade swept area. The results show that the convergence TBS (Type III) have a higher gap pressure between upstream and downstream, or they have best performance than other types.**

***Index Terms*—Simulation, tandem blade, savonius, turbine.**

I. Introduction

The Savonius hydrokinetic turbine is simple geometry and its construction is low-cost to manufacture. It starts rotating at lower speeds as compared to its counterpart hydraulic turbines, having a high starting torque. It produces low noise and can make use of the water river flowing in any horizontal direction to its rotation. However, in spite of these advantages, this turbine faces one main disadvantage of having low efficiency. This research paper aims to select the best design based on simulation investigation of the three models of Savonius Tandem Blade comprising Overlap TBS, Symmetrically TBS and Convergence TBS.

The Savonious conventional has two pairs of cylindrical blade that look like a letter S which not connected to the middle or with gaps (overlapping) on both ends of the blade that serves as the entry of outflow from the first blade (thrust) to the second blade (return). As shown in Fig. 1, the first blade (advancing blade) got a drag forces from the main flow (free flow) while the second blade (returning blade) got a returned forces opposite direction outflow through the gap (overlap) resulting in a pair of couple force that is able to generate torque and power.

Various approaches, with a variety of weightings of the parameters involved have been published in the literature. As seen as in Fig. 1, the conventional Savonius have parameters a and e are respectively $a = 0$ and $e = d/6$. The values of Power Coefficient (Cp) and Torque Coefficient (Cm) are experimentally determined as a function of the velocity coefficient (λ). Menet [1], [2] give a illustration of the pressure distributions and of the flow field inside the Conventional Savonius rotor for the optimal configuration $(e\text{-}e')/d$=0.242 which resulted an optimum Cm = 0, 33 as showed in Fig. 2.

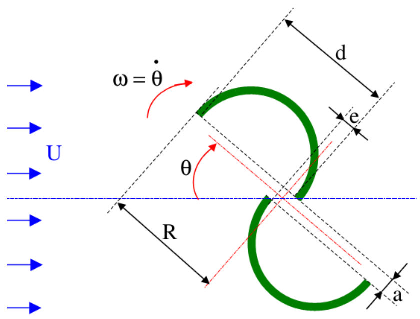

Fig. 1. Conventional Savonius Blade [1]

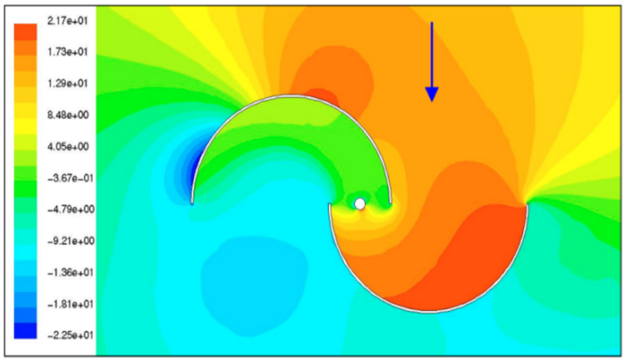

Fig. 2. Pressure distribution (Pascal) for $Re_D = 1.56 \times 10^5$ and $(e\text{-}e')/D$ = 0,242. [1]

Chauvin and Benghrib [3] presented the measurements of the pressure field method, leads to the determination of the lift and drag coefficients on the Savonius Rotor before software simulation has been popular like now. Pressure gauges are located into six circular holes in the mid-plane of the blade cross-section. The pressure gauges are of piezoresistive type with thermal compensation. The signals are first amplified on the top of the blade and then transmitted to the outer measurement chain by means of rotating contacts. Then they obtain the instantaneous pressure field on each side of a blade for a complete revolution of the machine. Pressure measurements have been performed for two sets of experiments; the first one for $U \approx 10$ m/s and the second one for $U \approx 12.5$ m/s. In each case it is to be noted that a negative lift effect is present for low values of the tip speed ratio λ. The lift coefficient becomes positive when λ increase. The drag coefficient is of course always negative.

Manuscript received November 29, 2012; revised February 11, 2013.
The authors are with the Mechanical Engineering Department, State Polytechnic of Malang. Indonesia (e-mail: baguspoltek@gmail.com, sudjitospn@yahoo.com, slamet_w72@yahoo.co.id, denny_malang2000@yahoo.com).

DOI: 10.7763/JOCET.2013.V1.65

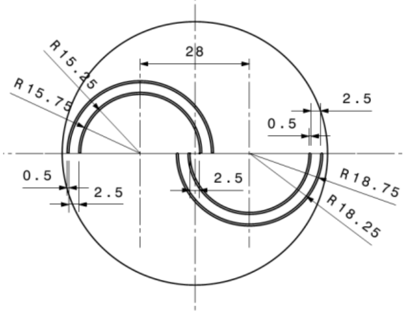

(a) Overlap TBS (Type I)

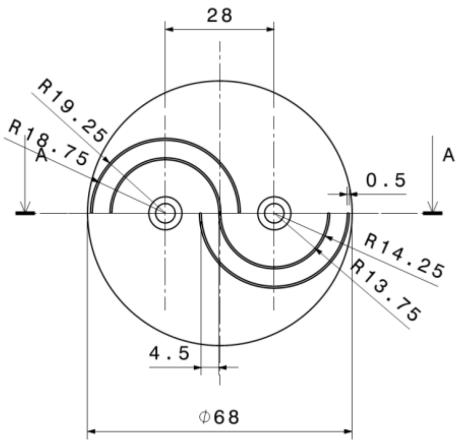

(b) Symmetrically TBS (Type II)

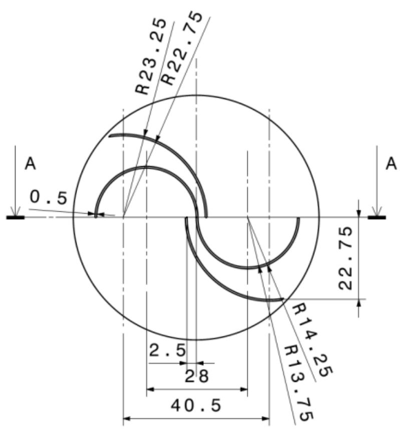

(c) Convergence TBS (Type III)

Fig. 3. Three types and dimension of Tandem Blade of Savonius (TBS) Design.

Currently, the Savonious turbine has been developed with various modified whose purpose is to improve their performances. Menet also modified the savonius rotor which only changes the position of an off-set the second pair of rotor blades, now has three geometric parameters, namely: (*1*) primary overlap (*e*), secondary overlap (*e*'), and the angle between the axis blades (β). The result is relatively hopeful as new rotor induces maximum value of static torque is much higher than those obtained with the conventional rotor. However, they found low values and the negative of torque where an angle β large variations. Overall, the average value of the torque increased to Cm = 0.48 or 60% more than the conventional rotor.

Fujisawa [4] has published a study comparing experimental results with a numerical study also using the discrete vortex method. He concluded that the numerical calculations were adequate to “predict the basic features of the variation in flow fields with rotor angle”. Nevertheless, the procreation of the flow field around a stationary rotor was poor, and Fujisawa supposed that it was due to false assumptions used in the calculations. Sometimes, some visualizations of the flow in and around the rotor are proposed, but with a poor description of the physical phenomena. But, Fujisawa [5], [6] presented a exclusive description of the Visualization study of the flow in and around a of the conventional Savonius rotor, they conclude that the pressure coefficient decreased overall due to the effect of the circulation generated by rotor rotation. Looks like this is a phenomenon circulation persists in revolving condition compared with stationary rotor, where the flow through the overlap is reduced due to backflow. The flow is expected to reduce the effect of pressure recovery on the back side of blade behind because of the pressure distribution near the overlap.

Kamoji et al. [7] improve the coefficient of power and to obtain uniform coefficient of static torque. To achieve these objectives, the rotors are being studied with and without central shaft between the end plates. Experimental tests in a closed jet wind tunnel on modified form of the conventional Savonius rotor with the central shaft were to have $Cp = 0.32$. They studied the effect of geometrical parameters on the performance of the rotors in terms of coefficient of static torque, coefficient of torque and coefficient of power. The parameters studied are overlap ratio, blade arc angle, aspect ratio, and Reynolds number.

Performance of Savonious hydro-kinetic turbine has dependence with the principle to generate drag forces is formulated by $F = p.\ A = ½.\ \rho.\ A.U^2$, thus optimizing torque and power turbine formation is highly dependent on the blades swept area (A) and velocity of fluid (U). Therefore, this paper introduced a new concept design of Savonius Tandem Blade by broadening swept area that can increase drag force production on the blade as shown as Fig. 3.

II. Method

By using simulation software ANSYS 13 it’s the following boundary conditions that have been applied. The stationary domain has a free stream velocity. The hydrodynamic pressure conditions are applied and the initialization is done. Inlet and Outlet are default boundary conditions in simulation software. Inlet requires the speed of inlet velocity of water and the outlet requires the relative pressure, 1.0132×10^5 Pa, at the initial conditions. The blade surfaces are enabled a “wall” condition. This condition enables the calculation of properties such as force, torque on the surface. Once the domains have been specified a default fluid-fluid interface is detected between the rotating and stationary domain.

A two-dimensional view of the rotor model was considered. It is because the rotor blade rotate in the same plane as the approaching water flow stream. The computational domain was discretisized using two-dimensional unstructured mesh (triangular mesh). The left boundary had Velocity Inlet condition while the right boundary had Outflow condition. The top and bottom boundaries for the open channel sidewalls had symmetry conditions. The moving wall condition was employed for the rotor model to study the effect of fluid motion in and around the rotating Savonius rotor. The dimensions of the computational domain were 500 mm in length and 75,5 mm in width, which were also similar to the experimental conditions. For the various model conditions, the geometry of the rotor was changed and accordingly different meshes were generated for each condition.

Steps in the simulation solutions are consist of:

1) Solver:
   - Solver: Pressure Based
   - Time: Steady
   - Space: 2D
2) Viscous Model:
   - Model: Standard k-epsilon (k-ε)
   - Near-Wall Treatment: Standard Wall Functions
3) Material:
   - Water (μ= 1.002x10^{-3} kg/m-s, ρ= 1.000 kg/m^3)
4) Operating conditions:
   - Atmospheric Pressure (1.0132 bar)
5) Boundary Conditions:
   - Inlet: Velocity Inlet
   - Sides: No slip wall
   - Blades: Stationary Wall
   - Outlet: Outlet
6) Solution controls:
   - Pressure Velocity Coupling: SIMPLE
   - Discretization: fluids
7) Pressure (Standard)
   - Inlet Velocity: 1 m/s

III. Results and Discussion

In the contour plots, the blade on the left hand side is the returning blade and that on the right hand side is the advancing blade. The contour plots predict the variations in velocity and pressure in various regions near the blades within the flow domain. It can be observed from the pressure contour plots that pressure drop occur across the rotor from upstream to downstream side. This pressure drop indicates power extracted by the rotor causing its rotation.

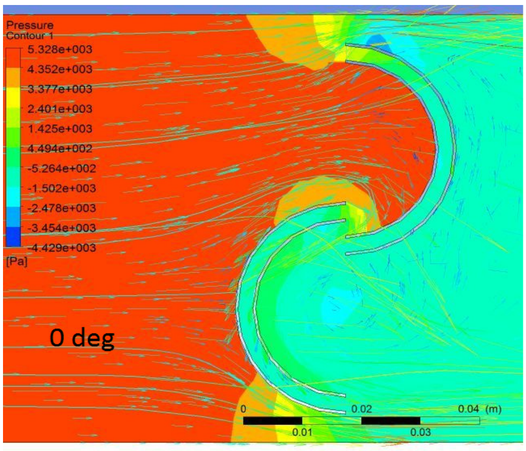

Fig. 4. Pressure distribution contour and streamline for overlap TBS (Type I) at 0° rotor angle.

The static pressure on the convex side of both the blades can be observed to be lower than those on the concave side of the blades; in fact, a region of negative pressure exists on the convex side of the blades. This occurs due to the high flow velocity over the convex side of the blades. As a result, a pressure difference acts across the concave and convex side of the blades, which provide the necessary torque for causing rotation of the blades. The maximum static pressure drop is found in type III at 0° rotor angle with downstream pressure is (-1.574e+003 Pa) see on Fig. 6, then followed type I and type II with downstream pressure is (-5.264e+002 Pa) and (- 6.426e+002 Pa) respectively see on Fig. 4 and Fig. 5.

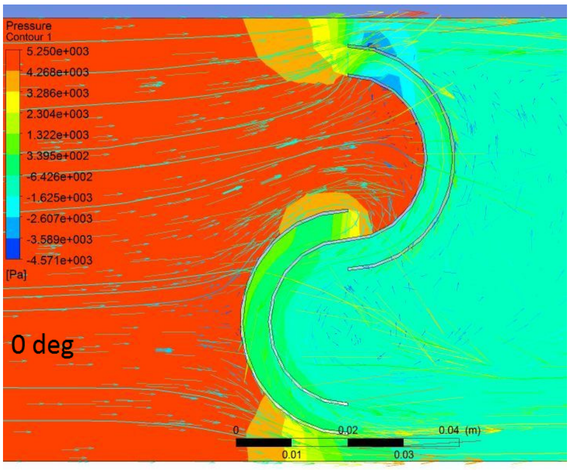

Fig. 5. Pressure distribution contour and streamline for Symmetrically TBS (Type II) at 0° rotor angle.

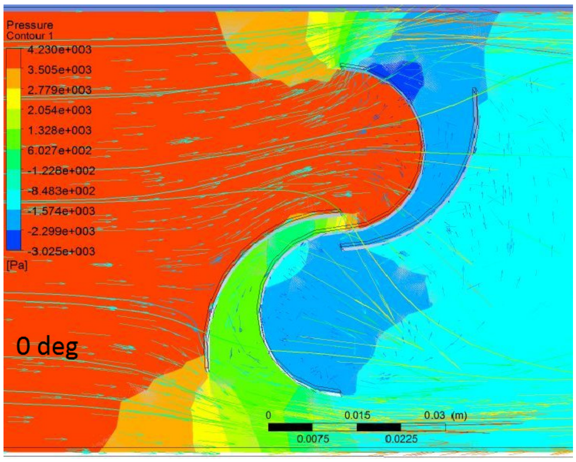

Fig. 6. Pressure distribution contour and streamline for Convergence TBS (Type III) at 0° rotor angle.

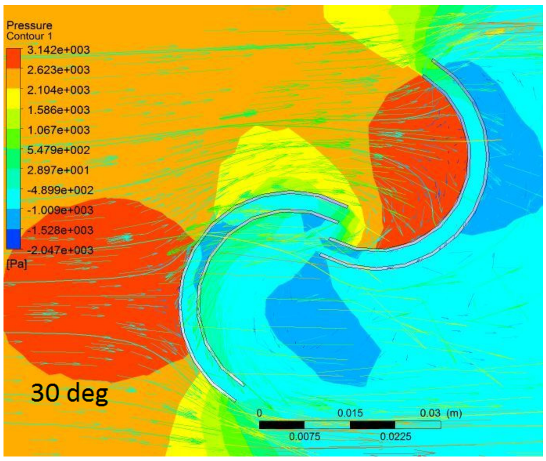

Fig. 7. Pressure distribution contour and streamline for Overlap TBS (Type I) at 30° rotor angle.

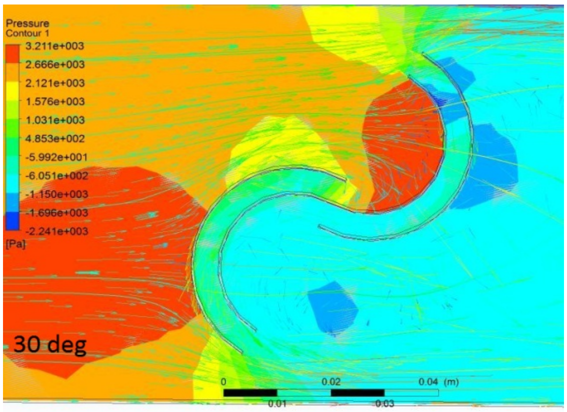

Fig. 8. Pressure distribution contour and streamline for Symmetrically TBS (Type II) at 30^o rotor angle.

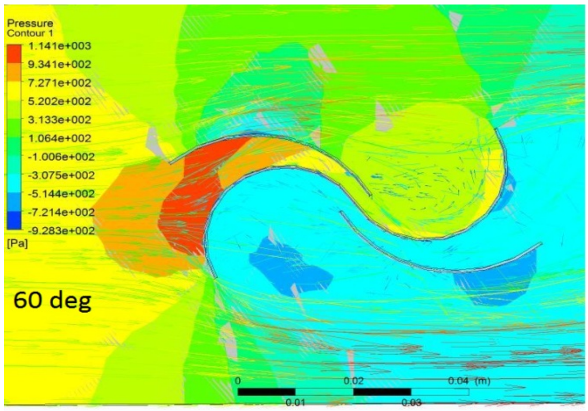

Fig. 12. Pressure distribution contour and streamline for Convergence TBS (Type III) at 60^o rotor angle.

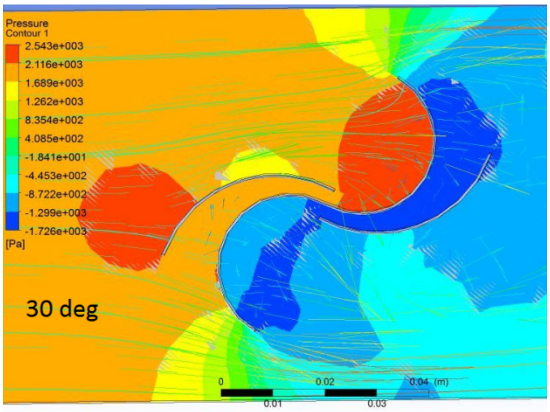

Fig. 9. Pressure distribution contour and streamline for Convergence TBS (Type III) at 30^o rotor angle.

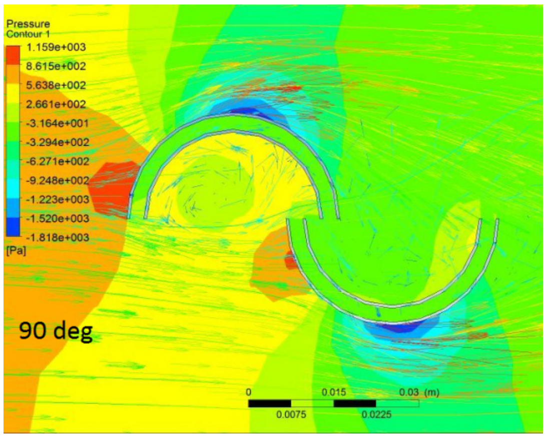

Fig. 13. Pressure distribution contour and streamline for Overlap TBS (Type I) at 90^o rotor angle.

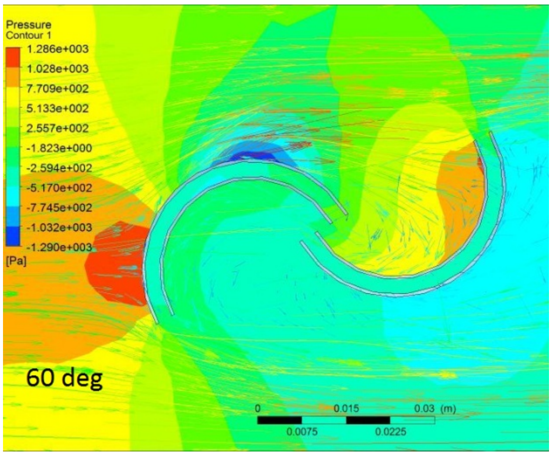

Fig. 10. Pressure distribution contour and streamline for Overlap TBS (Type I) at 60^o rotor angle.

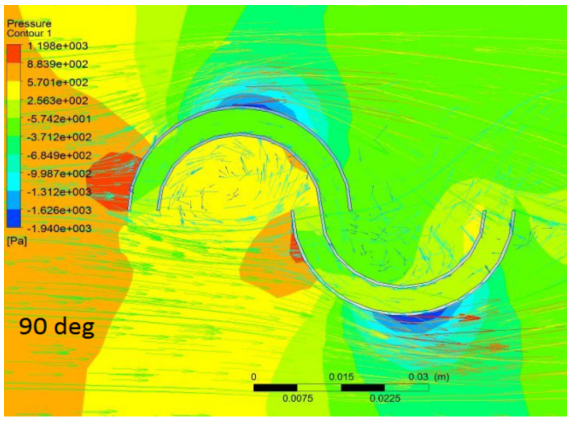

Fig. 14. Pressure distribution contour and streamline for Symmetrically TBS (Type II) at 90^o rotor angle.

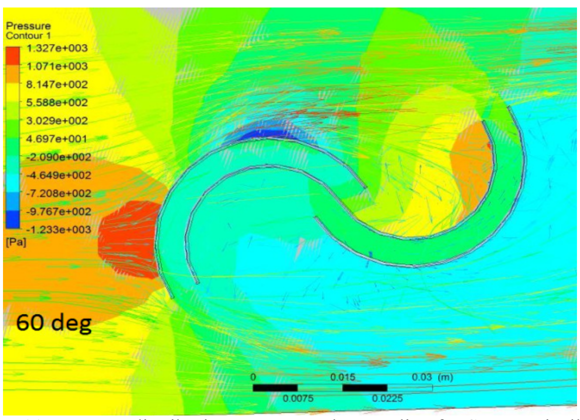

Fig. 11. Pressure distribution contour and streamline for Symmetrically TBS (Type II) at 60^o rotor angle.

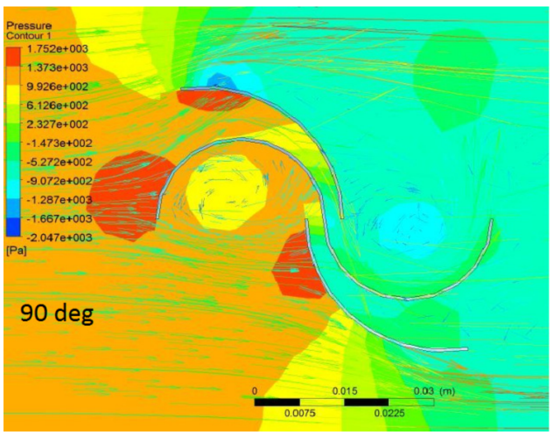

Fig. 15. Pressure distribution contour and streamline for Convergence TBS (Type III) at 90^o rotor angle.

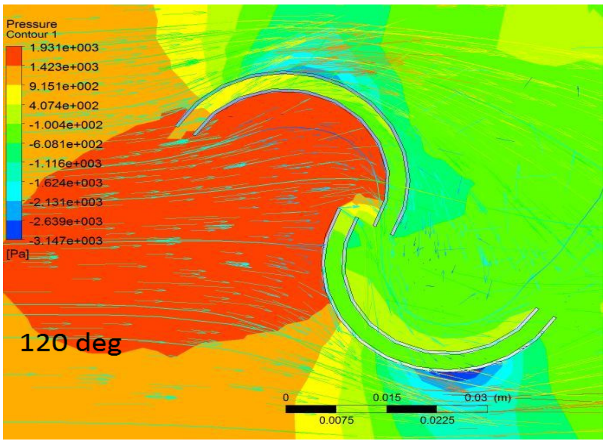

Fig. 16. Pressure distribution contour and streamline for Overlap TBS (Type I) at 120° rotor angle.

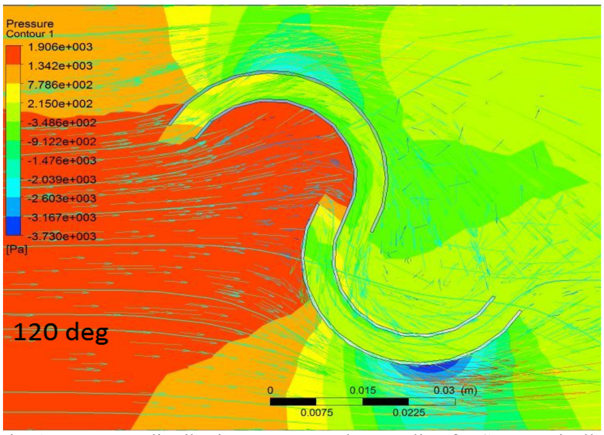

Fig. 17. Pressure distribution contour and streamline for Symmetrically TBS (Type II) at 120° rotor angle.

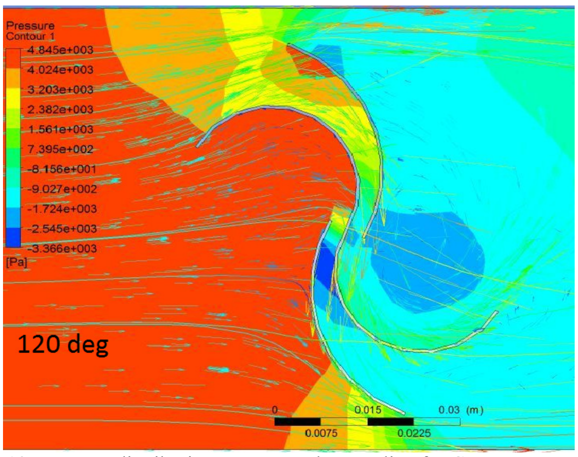

Fig. 18. Pressure distribution contour and streamline for Convergence TBS (Type III) at 120° rotor angle.

Role as an extra blade tandem to be returning blade began to look at the position in case of the rotor angle 30° and 60° using type III (Fig. 9 and 12), whereas in type I and II has not shown his role. At the position in case of the rotor angle 30° and 60° both of type I and II (Fig. 7, 8, 10 and 11) showing that returning blade still stuck by the dynamic pressure was derived from the free flow which potentially cause vibration due to the unbalance couple forces between the advancing blades and the returning blades. Then a stability will be obtained in case of convergence TBS and hence it will have minimum vibration during rotation.

At the position in case of the rotor angle 90° in type I and II parts of advancing tandem blade still have obstacles pressure on the convex side and also occurred the vortex flow on the concave side which would cause a vibration and energy loss (see Fig. 13 and Fig. 14). While for the type III at the same position of advancing blade rotor angle are ready to bring into being optimally drag forces (see Fig. 15). Finally at the position in case of the rotor angle 150° in type III achieving peak performance in producing the largest turbine power, the Fig. 18 and Fig. 19 shows the difference in pressure on the upstream (4.484*e* +003 *Pa*) and downstream (-2.545*e* +003 *Pa*) exceeds the performance of type I and type II in the same position.

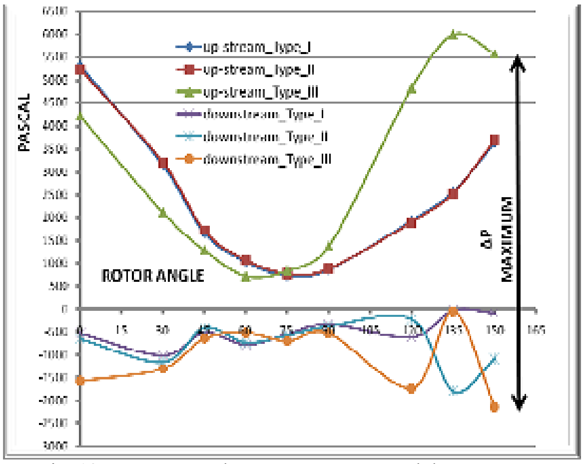

Fig. 19. Pressure gap between up-stream and down-stream

IV. Conclusion

From the present study, the following conclusions are summarized:

1) The best performance based on the maximum difference in pressure upstream and downstream is Type III (Convergence Tandem Blade of Savonius).
2) The maximum static pressure drop is found in type III at 150o rotor angle with downstream pressure is (-2.245e +003 Pa).
3) At the position of rotor angle 90° in type III, advancing blades is starting growth to produce optimally drag force. Then peak performance of convergence TBS is achieved when the rotor angle reaches 150°.

Acknowledgement

The authors acknowledge with thanks the assistance rendered by Dr. Eng. Agus Choiron, (Lecturer) and Tri Handoko (Assistant Lecturer), Manufacture and Engineering Design Laboratory Department of Mechanical Engineering, Brawijaya University of Malang - Indonesia), for providing crucial insights during the course of the research work.

References

[1] J. Menet. Increase in the Savonius Rotors Efficiency via a Parametric Investigation. [Online]. Available: http://www.2004ewec.info/files/23_1400_jeanlucmenet_01.pdf
[2] J. Menet, "Aerodynamic behaviour of a new type of slow-running VAWT," *Wind Energy Proceedings of the Euromech Colloquium, Springer*, vol. 43, pp. 235-240, 2007.
[3] A. Chauvin and D. Benghrib, "Drag and lift coefficient evolution of a Savonius Rotor," *Experiments in Fluids*, vol. 8, 1989, pp. 118-120.
[4] N. Fujisawa, "Velocity measurements and numerical calculations of flow fields in and around Savonius rotors," *J. Wind Eng. Ind. Aero*, vol. 59 1996, pp. 39-50.

[5] N. Fujisawa and F. Gotoh, "Visualization study of the flow in and around a Savonius rotor. Experiments in Fluids," vol. 12, no. 6, pp. 407-412, 1992.
[6] R. Gupta *et al*., "CFD Analysis of Two bucket Savonius Rotor for Various Overlap Conditions," *ISESCO Journal of Science and Technology*, vol. 8, no. 11, 2012, pp. 67-74.
[7] M. A. Kamoji, S. B. Kedare, and S. V. Prabhu, "Experimental investigations on single stage modified Savonius rotor," *Applied Energy*, vol. 86, no. 7-8, pp. 1064-1073, 2009.

Bagus Wahyudi is Bachelor of Mechanical Engineering, National Institute of Technology (ITN), Malang – INA, 1981. Master of Mechanical Engineering, Sepuluh Nepomber Institute of Technology (ITS), Surabaya – INA, 2007. Pursuing Doctoral Degree in Mechanical Engineering Post Graduated Program of Brawijaya University (UB) Malang-INA, since 2011. He work as lecturer at Mechanical Engineering Department, State Polytechnic of Malang INA since 1983 until now.

Sudjito Soeparman is Bachelor of Mechanical Engineering, Sepuluh Nopember Institute of Technology (ITS), Surabaya – INA, 1974. Ph.D in Mechanical Engineering, The University of New South Wales-Sydney Australia, 1998. He works as Professor at Mechanical Engineering Department, Brawijaya University of Malang INA since 2003 until now, joint with Mechanical Engineering Post Graduated Program in Energy Conversion Field of Research. He is the former of Dean in Engineering Faculty of Brawijaya University. His research interest is the new of Renewable Energy.

Denny Widhiyanuriawan is Bachelor of Mechanical Engineering, Brawijaya University, Malang – INA, 1998. Master of Mechanical Engineering, Gajahmada University, Jogyakarta – INA, 2003. Doctoral Degree in Geoinformatics Engineering Post Graduated Program of Pukyong National University, South Korea, 2011. Work as lecturer at Mechanical Engineering Department, Brawijaya University of Malang INA since 2000 until now, joint with Mechanical Engineering Post Graduated Program as Assistant Professor in Energy Conversion Field of Research. He is member of the Korea Institute of Maritime Information & Communication Science. His research interest: Geoinformatics Engineering and The new of Renewable Energy.

Slamet Wahyudi is Bachelor of Mechanical Engineering, Brawijaya University, Malang – INA, 1995.Master of Mechanical Engineering, Sepuluh Nopember Institute of Technology, Surabaya – INA, 2003. Doctoral Degree in Biomedical Engineering Post Graduated Program of Brawijaya University, INA, 2006. Work as Head of Mechanical Engineering Department, Brawijaya University of Malang INA since 2007 until now, joint with Mechanical Engineering Post Graduated Program as Assistant Professor in Energy Conversion Field of Research. His research interest: The new of Renewable Energy.